Mine Water Environ (2017) 36:114–123
DOI 10.1007/s10230-016-0419-z

TECHNICAL ARTICLE

Predicting Open Pit Mine Inflow and Recovery Depth in the Durvuljin soum, Zavkhan Province, Mongolia

Yohannes Yihdego[1] · **Andrew Paffard**[1]

Received: 28 July 2015 / Accepted: 16 September 2016 / Published online: 26 September 2016

Abstract Increasingly, mine issues and water resources are being managed on a watershed basis, while addressing problems at the local mine scale. A good example of this developed when empirical and analytical modelling of the potential inflow to an open pit mine in the Durvuljin soum, a region in northwest Mongolia, indicated that inflow would be on the order of 0.3 to 10.5 L/s. In this study, the radius of influence due to open pit mining was estimated to be between 0.6 and 3 km. Based on simulated drawdown contours and transient pit inflow figures that captured the impact of mining and groundwater inflow rate variations over a period of time, it appeared that advanced dewatering will not be required at this mine, unless currently unknown major fractured structures are intercepted. In-pit basal sumps and pumps should be sufficient to remove water from the mine floor. However, an assessment of the final pit level is also crucial to planning the post-mining surface and groundwater quality/eco-system and mitigation requirements during recovery. Our post-mining water table recovery estimate indicated that inflow will exceed evaporation and that a shallow lake will likely form. While such solutions, which do not rely on complex numerical models nor excessive input data, are not appropriate for all hydrogeologic situations, they are relevant to the conditions encountered at most mine sites.

Keywords Pit lake · Post-closure · Mine rebound · Mine water management

✉ Yohannes Yihdego
yohannesyihdego@gmail.com

[1] Snowy Mountains Engineering Corporation (SMEC), Sydney, NSW 2060, Australia

Introduction

Predicting the amount of water inflow into a pit is very important for development of a mine dewatering program. Hydrogeological analytical models are frequently used for this purpose and many analytical solutions for predicting water inflow into mine excavations can be found (e.g. Rupp et al. 2009). These models were often developed based on very specific assumptions and boundary conditions that restrict their applicability. Numerical methods have been used to deal with complex mining situations (Li et al. 2011; Mengistu et al. 2015; Singh and Woolhiser 2002; Voss 2011) and graphical tools that facilitate the construction of complex models have been developed as computers have become more powerful and groundwater flow codes have become more standardized (Bredehoeft 2005; Kazemi 2012; Vandenbohede et al. 2011). However, the trend toward larger models and increased model complexity is not necessarily improving our understanding of the natural system.

Predicting groundwater inflow into the pit over time is typically required to simulate the effects that mining and concomitant groundwater extraction will have on an area's regional groundwater system (Rapanova et al. 2007; Sloan 2000; Tammetta 2013). Regulators need to know that mining operations will not jeopardise groundwater extraction for water supply purposes at other sites in the region. Much attention has been paid in recent years to improving our ability to model localized effects and complex hydrogeological processes, but although some problems clearly require complex models, in many instances, a simplified model can be used to meet model objectives (Toran and Bradbury 1988; Wu 2013). When used for scoping calculations or to test conceptual models, simple techniques are often more robust and better suited for more sophisticated calibration techniques, such as parameter estimation. Paradoxically, reducing model complexity can also increase the modeller's understanding of the groundwater flow system.

The objectives of this study were to assess groundwater inflows to open mine pits and predict final pit void water levels at an open pit mine in the Durvuljin soum, a region in northwestern Mongolia. The data and our interpretations have been sourced from consultant reports by SMEC (2011, 2012).

Study Area

The study area is 930 km west of Mongolia's capital city, Ulaanbaatar. The project area, located in the semi-desert zone of the Great Lake lowlands of northwest Mongolia, is mountainous with elevations ranging between 1670 and 2160 m above sea level (asl). The mine sites are at an average elevation of about 1780 m and the entire area drains south towards the Zavkhan River some 22 km away (Fig. 1).

Average total annual precipitation for the past 10 years was only 90 mm, while the long term average was 130 mm, of which 90% falls during summer. Rainfall is often observed falling on the higher hills around the mine while not elsewhere (Hasiniaina et al. 2010).

The geological strata of the area consist of green schist facies, meta-volcanics, marble, sandstone, and limestone. In the central part of the ore deposit, water-bearing middle Riphean Shuvuun Formation shale was intersected at depths between 60 and 90 m (Battumur 2009). The other principle aquifer in the area is the colluvial unconsolidated sediment, which is distributed near the slopes of mountains and through the ravines and dry river beds. It consists of gravel and pebbles, small clay lenses, and small boulders. Recharge is limited in the mineralised zones; low-yielding bedrock aquifers are found in this formation.

Method

Hydrogeological Site Assessment

A hydrogeological assessment was conducted based on information obtained from a drilling and aquifer testing programme (to assess geology, aquifer thickness, permeability, transmissivity, water quality, areal extent, and vertical leakage). Monitoring boreholes (Fig. 1) ranging in depth between 25 and 120 m were installed to assess groundwater conditions surrounding and within the proposed pit.

An induced polarization (IP) survey was conducted by GeoMaster Engineering LLC. Five lines totalling 24,000 m were surveyed using 100 m dipole spacing. A QGX Mongolia LLC geologist calibrated the data and used existing boreholes to provide a depth to basement and to contour the basement profile.

Work conducted in 2012 provided additional information on the hydrogeology of the pit area. Of the 14 monitoring wells, recovery tests were conducted on eight, of which four yielded useful results. In addition, the local potentiometric surface was better defined (Fig. 2) and showed that groundwater flows to the south. This reflects the topography and relative proximity to recharge areas in the higher hills north of the mine (SMEC 2012).

Hydraulic Properties

Data loggers were installed in selected boreholes around the proposed pit and the bore was airlifted for 20 min, with subsequent water level recovery recorded by an electronic data logger. The data were subsequently processed and interpreted using Aqtesolv Pro 4.0® software. The Barker Method (Barker 1988) was used to assess permeability ranges. The aquifer properties adopted in this study were based on the results of the hydrogeological investigation (recovery tests) and data contained in Li et al. (2011).

Monitoring bores, recovery testing, survey of the measuring points, and water level monitoring indicated:

- a regionally extensive low permeability water table aquifer;
- recharge is from the north, with discharge to the south, most likely at the Zavkhan River;
- the gradient is steep with a higher gradient north of the mine (0.08) and a lower gradient to the south (0.03); the average regional gradient is about 0.02; and
- aquifer transmissivity ranges between 4 and 6 m^2/day. Storage coefficient value ranges between 0.01 and 0.0001.

Also, the following assumptions were made:

- the pit will be 100 m deep with a diameter of 500 m;
- the water table will be intersected by the pit at 60 m beneath the surface; and
- the water-bearing fractured rock zones are flat-lying, uniform, and not extensive, and are only located on the northern and eastern sides of the pit.

Figure 3 shows the conceptual model. Groundwater flow is predominantly perpendicular to the axis of the mine area. This boundary was assumed to have no flow; errors in this assumption are likely to have a minimal effect on salient model predictions due to the distance between the mine (and any locations where the mine will have significant hydraulic influence) and the boundary.

Analytical and empirical methods were used to simulate the interaction of the proposed mine with the groundwater system of the mine area.

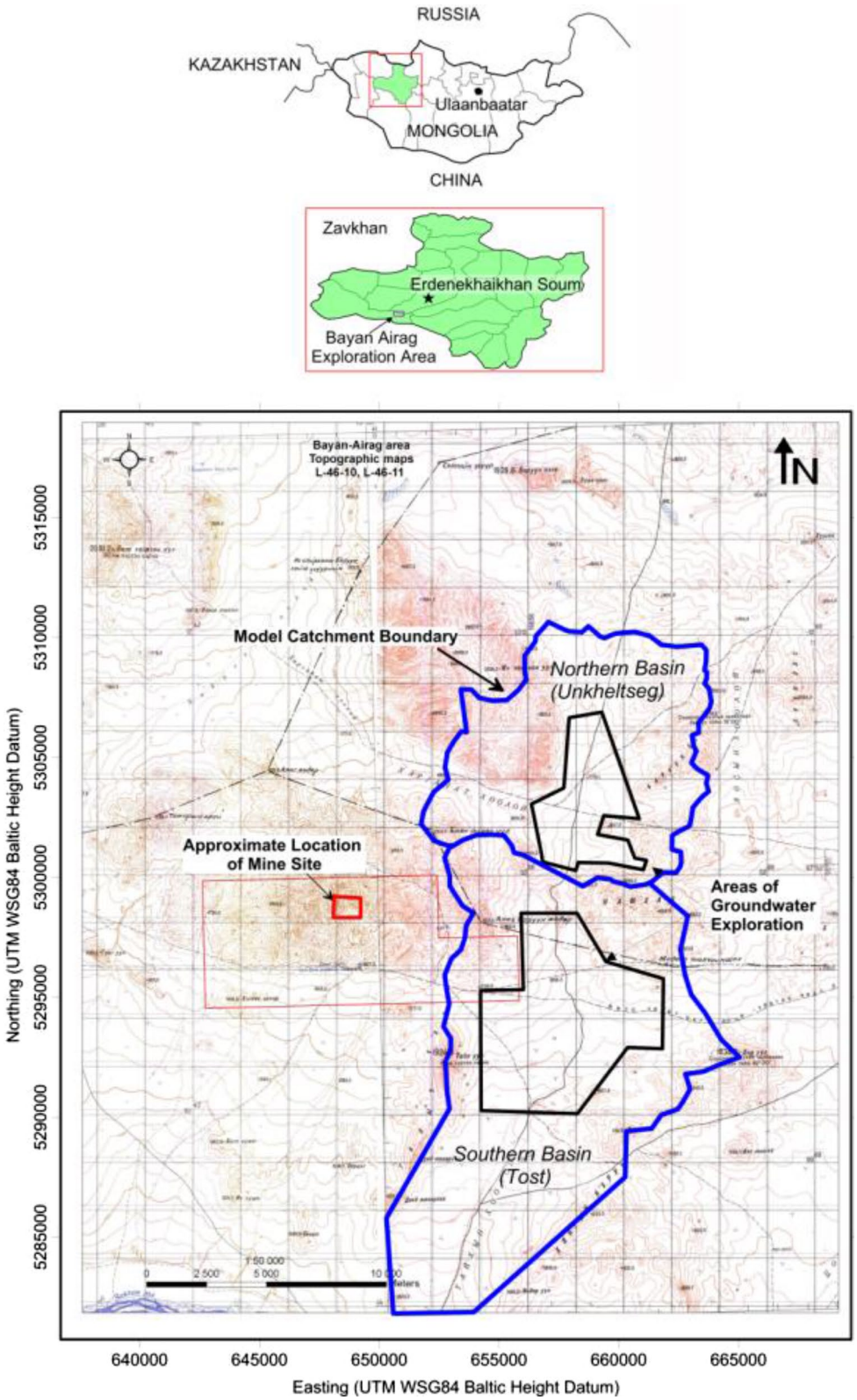

Fig. 1 Study area, with the mine area labelled as a rectangular line (after Yihdego et al. 2015)

Long-Term Pit Inflow Estimation

The conceptual flow model for the assessment of pit groundwater inflow (Fig. 3) was approximated by an analytical model (Marinelli and Niccoli 2000; Eq. 1). The conceptual model was divided into two zones: Zone 1 lies above the base of the pit and represents flow to the pit walls, and Zone 2 extends from the bottom of the

pit downward and considers flow to the pit bottom. The analytical models assumed that there was no groundwater flow between Zones 1 and 2.

The steady state analytical solution considers the effect of decreased saturated thickness near the pit walls, distributed recharge to the water table, and upward flow through the pit bottom, with the following assumptions:

Zone 1 Analytical Solutions

- The pit walls were approximated as a vertical-walled circular cylinder;
- groundwater flow is horizontal (Dupuit-Forchheimer approximation is valid);
- the static (pre-mining) water table is horizontal;

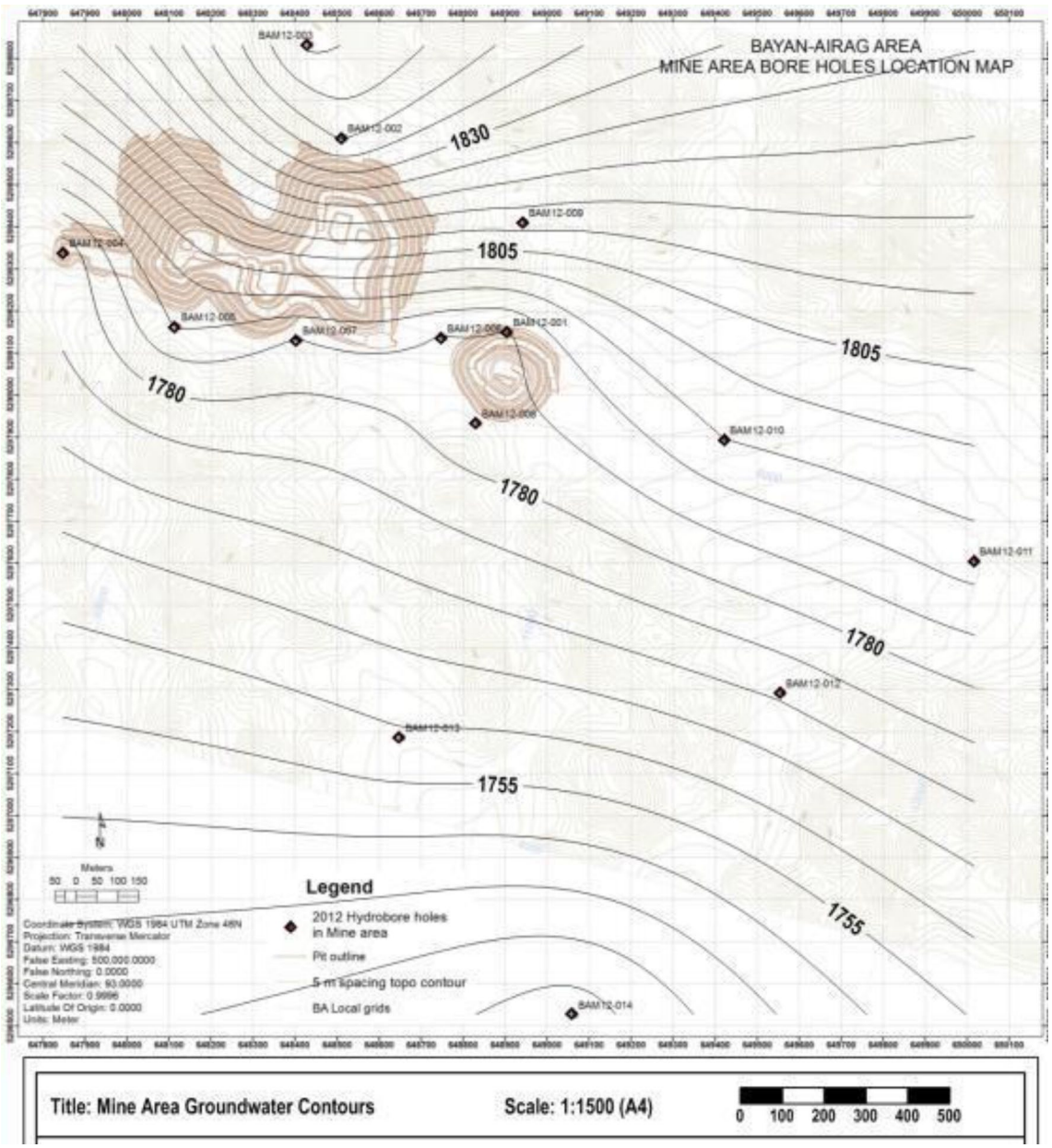

Fig. 2 Groundwater contour map, including location of the mine area's borehole locations

- groundwater flow toward the pit is axially symmetric;
- uniformly distributed recharge occurs across the site as a result of surface infiltration; and
- all recharge in the radius of influence is captured by the pit.

Zone 2 Analytical Solutions

- The hydraulic head is initially uniform throughout the zone. The initial head is equal to the elevation of the initial water table in Zone 1;
- the disk (conceptual base of the pit) sink has a constant hydraulic head equal to the elevation of the pit lake water surface. If the pit is dewatered, the disk sink head is equal to the elevation of the pit bottom; and
- flow to the disk sink is three dimensional and axially symmetric.

Equation 1 applies for these conditions:

$$h_o = \sqrt{h_p^2 + \frac{W}{K_{h1}}\left(r_o^2 \ln\left(\frac{r_o}{r_p}\right) - \left(\frac{r_o^2 - r_p^2}{2}\right)\right)}$$
$$Q_1 = W\pi\left(r_o^2 - r_p^2\right)$$
$$Q_2 = 4r_p\left(\frac{K_{h2}}{m_2}\right)\left(h_o - d\right) \quad (1)$$
$$m_2 = \sqrt{\frac{K_{h2}}{K_{v2}}}$$

where: W = the distributed recharge flux; K_{h1} = the horizontal hydraulic conductivity of materials within Zone 1; K_{h2} = the horizontal hydraulic conductivity of materials within Zone 2; K_{v2} = the vertical hydraulic conductivity of materials within Zone 2; r_p = the effective pit radius; m_2 = an anisotropy parameter; d = the depth of the pit lake; h_p = the saturated thickness above the base of Zone 1 at r_p (that is, the saturated thickness at the pit wall); r_o = the radius of influence (maximum extent of the cone of depression); Q_1 = the pit inflow rate from zone 1 (through the pit wall); and Q_2 = the pit inflow rate from zone 1 (through the pit bottom).

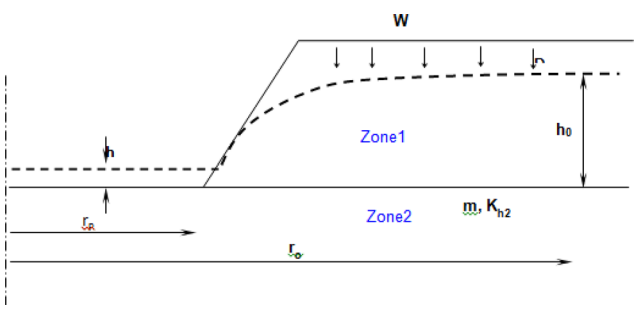

Fig. 3 Pit inflow idealized analytical model

Hydraulic head contour lines within the Zone 2 region were computed from Eq. 2, which incorporates coordinate transformations for anisotropy (Marinelli and Niccoli 2000).

$$H_2(r,z) = H_0 - 2\frac{(h_0 - d)}{\pi}\sin^{-1} \times \left\{\frac{2r_p}{\sqrt{\left(\left(r - r_p\right)^2\right) + \left(m_2 z\right)^2} + \sqrt{\left(r + r_p\right)^2 + \left(m_2 z\right)^2}}\right\} \quad (2)$$

where: H_2 = the hydraulic head elevation within Zone 2; r = the radial distance from the center of the pit, and z = the vertical depth below the pit bottom (positive downward).

The 'radius of influence' is defined as the maximum distance at which the drawdowns can be detected with typical field technology (Dragoni 1998; Soni et al. 2015). The most common way to find the radius of influence is by using an empirical formula, such as the Sichardt formula (Eq. 3), but the radius value for this formula is the smallest one and represents 40 % of the maximum drawdown. Thus, the Sichardt radius value can't match the radius of influence definition. Dispersion of the radius of influence values reveal the empirical nature of formulas that depend only on the parameters considered.

$$r_o = 3000\,(H - h_w)\sqrt{k} \quad (3)$$

where: r_o = the radius of influence (m); (H−hw) is the drawdown (m); and K is the soil/aquifer hydraulic conductivity in m/s. The radius of influence was calculated using Eq. 3 (considering the symmetrical flow from the other side) plus the radius of the pit, which is the effective radius. Due to asymmetric flow, the estimated radius of influence was doubled, considering the site-specific knowledge of the area. A plot of drawdown versus the radius of influence (using Eq. 3) and a range of hydraulic conductivities (0.002–2.0 m/day), are shown in Fig. 4.

The radius of influence estimated using Eq. 3 was further used to optimize the storage coefficient, by iteration to match with the time variant radius of influence calculated using Eq. 4.

$$r_o = 1.5\,(\sqrt{K \times b \times t \div S}) \quad (4)$$

where: b is the saturated aquifer thickness (m); t is time; and S is the storage coefficient. The radius of influence at any time t is the radius at which the drawdown is zero. From Eq. 4, it can be seen that the radius depends only on time, transmissivity and storage coefficient and is completely independent of discharge rate. The discharge rate determines

the magnitude of the drawdown within the cone of depression, but not the areal extent. As long as it is used with care and common sense, this is a good approach to estimate the radius of influence, and provides a reasonable approximation, even for non-porous aquifers.

Alternative Long-Term Inflow Estimation

The inflow to the pit using Eq. 1, was cross-checked using the Thiem Eq. 5:

$$T = \frac{Q}{2\pi\left(h_2 - h_1\right)} \times ln\left(\frac{r_2}{r_1}\right) \tag{5}$$

where: T is aquifer transmissivity (m^2/day); Q is discharge rate (m^3/day); h_1 is the head at distance r_1 from the centre of the pit (metres); and h_2 is the head at distance r_2 from the centre of the pit (in metres).

Transient Pit Inflow Estimation

The time variant for a partially pit inflow was estimated using Eq. 6:

$$Q = \frac{\pi \times K \times \left(h_o^2\right) - \left(h_{pit}^2\right)}{ln\left(\sqrt{\left(\frac{(2.25 \times K \times h_o \times t}{S}\right)} \times r_e\right)} \tag{6}$$

where: h_o is the initial (pre-mining) saturated thickness above the base of zone; h_{pit} is the (post-mining) saturated thickness above the base of zone; and r_e is the effective radius (of the pit).

Long-Term Pit Water Balance

The pit water balance was used to calculate the final stage of the pit lake as it fills, accounting for precipitation and evaporation at the pit/lake surface, and groundwater inflow was estimated using Eq. 7, assuming nil contribution from overland runoff:

$$\Delta S = \left(\left(P - ET\right) \times A\right) + G_i \tag{7}$$

where: ΔS is the change in pit storage; P is precipitation (m/year); ET is the evaporation (m/year); A is the pit area (m^2); and G_i is the groundwater inflow (m^3/year). The change in water level (ΔL) in the pit is related to change in storage (ΔS) by (Eq. 8):

$$\Delta L = \left(\frac{\Delta S}{A \times S_y}\right) \tag{8}$$

where: ΔS is the change in pit storage; Sy is the specific yield of the pond at the relevant horizon; and A is the pit area (m^2). The Sy was assumed to be 1. The change in water level could be higher if the Sy is less than 1.

Analytical Groundwater Modeling

Assessment of the drawdown to the proposed open pit was carried out using the Analytical Aquifer Simulator (AnAqSim™) software. AnAqSim employs the analytic element method (AEM), which superimposes analytic solutions to yield a composite solution consisting of equations for head and discharge as functions of location and time. AnAqSim uses a variation of the AEM that divides the modelled region into subdomains, each with its own definition of aquifer parameters and its own separate AEM model (Fitts 2010). This subdomain approach allows for a high degree of flexibility with respect to a model's heterogeneity, anisotropy, and layering.

Model Performance

Hydraulic conductivities between 0.2 and 0.002 m/day were estimated by interpreting pump test data. Anisotropy was assigned by assuming a conductivity in the vertical

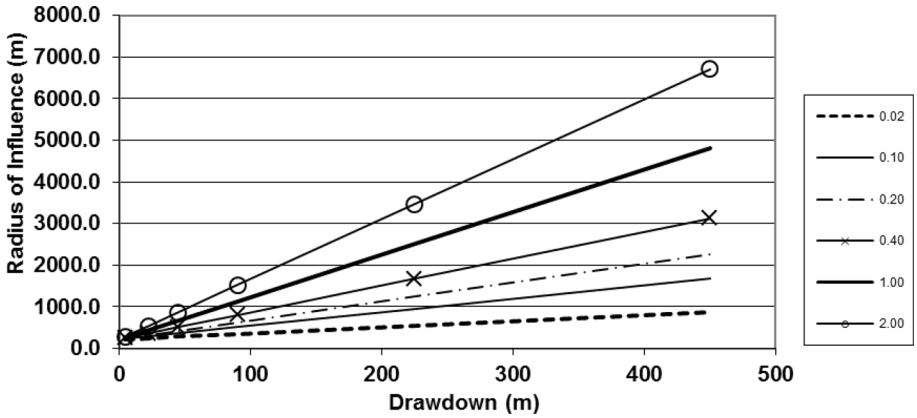

Fig. 4 Radius of influence versus drawdown

direction as being 1/10 of the horizontal conductivity. Storage coefficient values between 0.01 and 0.0001 were calculated based on pump test interpretation. The effects of uncertainty in hydraulic properties were tested by varying hydraulic conductivity and storage coefficient values. Long-term and transient pit flow over the lifetime of the mine pit, pit height, and the distributed recharge as 5 % of the rainfall fraction (long term average) were estimated.

Model calibration was undertaken using trial and error and Solver (iterations) using Excel™. The radius of influence were estimated and cross-checked using analytical and empirical methods, while, storage values were optimized to match the estimated radius of influence using the different methods (Eqs. 3 and 4), and indirectly constrained by the pumping test results. The optimized parameters from the long-term groundwater inflow computation were used for a transient prediction and long-term pit water balance calculation.

Attributes including the surface ground level, observed depth to water level, base of the pit (bottom), depth below the water level, and recharge were incorporated for the analytical computation (Eq. 1). Long-term pit inflow (Eq. 1) was computed using the procedure below:

Step 1: Calculate h_o using an assumed radius of influence;

Step 2: Iterate to determine the radius of influence until it calibrates the standing pit water level (h_o);

Step 3: Calculate pit inflow rate from zone 1 (using effective pit radius and radius of influence);

Step 4: Calculate pit inflow rate from Zone 2 (using the horizontal and vertical hydraulic conductivity). The conductivity in the vertical direction was assigned one order of magnitude lower than in the horizontal direction; and Step 5: Calculate total pit inflow.

Model Results and Analysis

The groundwater inflow and the post-mining water level drawdown were estimated using the methods described above. The model results are shown in Tables 1, 2 and 3, based on:

- the pit geometry (500 m × 300 m);
- ground level (1850 m asl);
- assumed depth to water level (30 m on average);
- base of the pit (1775 m asl), the pit is 122 m deep;
- depth below water level (55 m); and the
- long-term annual rainfall (130 mm).

Tables 1, 2 and 3 will be placed near here by the printer.

Long-Term Pit Inflow

Based on the Zone 1 and Zone 2 analytical solutions, it can be seen that the pit wall and pit bottom inflow rates (Q1 and Q2, respectively) are sensitive to the assumed bulk hydraulic conductivity. For the best estimate of hydraulic conductivity using the field pumping test data, the total inflow rate using Eq. 1 (Marinelli and Niccoli 2000) was computed to be 1.60 L/s. The proposed pits will be excavated to 55 m below the initial water table in a very low hydraulic conductivity host rock. Recharge in the area is low due to the high evaporation rate, and the water source for the pit inflow is mainly stored groundwater. Excavation of the pit was simulated as a one-time excavation at the first time step of the simulation.

An assessment of the radius of influence was extremely helpful for integrated mine planning and to achieve a target production economically without interruptions. The minimum and maximum estimated radius of influence (Eq. 3) ranged between 0.6 and 3 km, using a range of hydraulic conductivity values of 0.2 to 0.002 m/day (Table 1). The estimated long-term pit inflow ranged between 0.3 and 10.5 L/s using the estimated radius of influences and hydraulic conductivities. Note that the range of hydraulic conductivity values (Table 1) and storage coefficients (Table 2) were incorporated to analyse the degree of uncertainty with the data set of the hydraulic parameters.

Pit Inflow Estimate Versus Time

A transient simulation of mine inflows was estimated to predict flow to the mine; this simulation can include planned pre-drainage schemes. Table 2 shows the rate of inflow into the pit over the life of the mine for an assumed storage value of 0.01 to 0.0001. Also shown are make-up water extraction rates over this same period (Fig. 5), although initial inflows may be much higher until equilibrium is reached, or if structures are intersected that can transmit water from greater distances.

Final Pit Void Water Level

Pit water balance computation (Eq. 7), was used to assess if there was a deficit in volume or any pit lake rebound (Eq. 8). Equation 1 (Marinelli and Niccoli 2000) is the preferred choice for a long-term estimate of pit inflows since it considers a distributed recharge to the water table and accommodates upward flow through the pit bottom. The final pit water/lake level was estimated to be between 0.13 and 2.0 m deep (Table 3). This assumes a flat base to the pit; however, in reality the base of the pit will not be flat and only a small portion will be at 1775 m asl. Therefore, the flooded depth is likely to be higher than indicated. Depending on the permeability used, the volume of water in the pit (ΔS) may vary by an order of magnitude. The specific yield (Eq. 8) was assumed to be 1. The change in water level could be greater if the specific yield is less than 1 (if there is a refilling of materials including

Table 1 Range of long term (steady)-pit inflow and radius of influence by varying the hydraulic conductivity (K) values

Zone 1, pit wall	Zone 2, pit bottom		Recharge[a] (mm/year)	Radius of influence[b]	Q_2 (zone 2) L/s	Q_1 (zone 1) L/s	Q_T (total) L/s
Kh1	Kh2	Kz2					
0.02	0.02	0.002	8	1264	1.24	0.32	1.6 (140 m^3/day)
0.2	0.2	0.02	8	3010	7.3	3.2	10.5 (980 m^3/day)
0.002	0.002	0.0002	8	615	0.25	0.03	0.3 (26 m^3/day)

[a]A distributed recharge of 6% of the annual rainfall (which is 8 mm/year) directly into the pit area was assumed

[b]Radius of influence was estimated from iterative application of analytical and empirical methods and was constrained by the extent of the watershed divide

waste rocks and excavated soils). Therefore, it might be worthwhile to consider various values of specific yields to deal with the rebound prediction, given that discharges of polluted water from abandoned mines are a major cause of degradation of water resources. It should also be noted that the average annual precipitation used was 130 mm. Should the annual precipitation increase, the level of the water in the pit will also increase. Also, the volumetric runoff inflow from the adjacent watershed/basin feeding into the mine was assumed to be nil.

Table 2 Summary of time-based groundwater inflow (over 20 years)

Time (days)	Inflow (m^3/day)-storage = 0.01	Inflow (m^3/day)-storage = 0.0001
219	–	56
365	582	51
730	225	44
1095	166	41
1460	140	39
7300	74	32

Prediction of Drawdown in a Post-mining Scenario

To present the long-term impact to the water table, the drawdown after mining has ceased was estimated using the Analytical Aquifer Simulator (AnAqSim) model (Fitts 2010). This model assumes a uniform isotropic aquifer and uses the borehole monitoring results to provide the initial conditions. The aquifer properties were the same as those used in the pit inflow estimation. The greatest drawdown will occur north of the main pit and will be concentrated in the drainage line leading into the pit (Fig. 6).

With low permeability and/or recharge, the areal extent of the water table depression due to mine dewatering within the fractured rock is significant. Over the range of parameters used in the analytical and empirical equations, it was noted that the drawdown distribution near the mine was relatively insensitive to the aquifer transmissivity and recharge rate. Impacts downgradient of the pit (South) will be minimal, with a maximum drawdown of the water table of about 34 m at the pit. The impact margin (0 m drawdown) will be about 2 km to the south. This assumes that the fractured rock systems are not areally extensive or hydrologically disconnected (that the fractures do not extend to the base of

Table 3 Long term pit water balance

Water balance components	Evaporation[e]	Rainfall	Groundwater inflow	Change in storage (ΔS)[c]	Change in pit water level[d] (m)	Remark
mm/year	325	100				
m^3/year	48,750	19,500	49,086	19,836	0.13	Scenario 1[a]
m^3/year	48,750	19,500	331,600	302,350	2.0	Scenario 2[b]

[a]Scenario 1 (baseline-Kh = 0.02): The balance is not in deficit. There will be shallow pit lake, indicating the water will not be entirely consumed by evaporation. (The pit level will rise to 0.13 m)

[b]Scenario 2 (baseline- Kh = 0.2): The balance is not in deficit. There will be shallow pit lake, indicating the water will not be entirely consumed by evaporation. (The pit level will rise to 2 m)

[c]Change in storage (ΔS) was computed using Eq. 7 in m^3/year

[d]The change in water level (ΔL) was computed using Eq. 8 in m

[e]Evaporation was estimated from Sellers et al. (1995); aridity index map (whereby the ratio of precipitation/potential evaporation in the study area is ≈0.4)

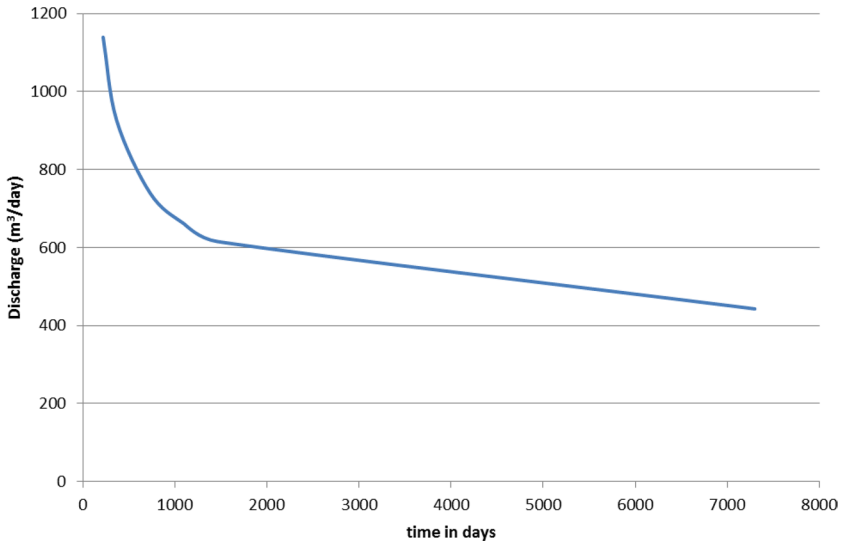

Fig. 5 Estimated pit inflow versus time, using a storage coefficient of 0.01 (Table 2)

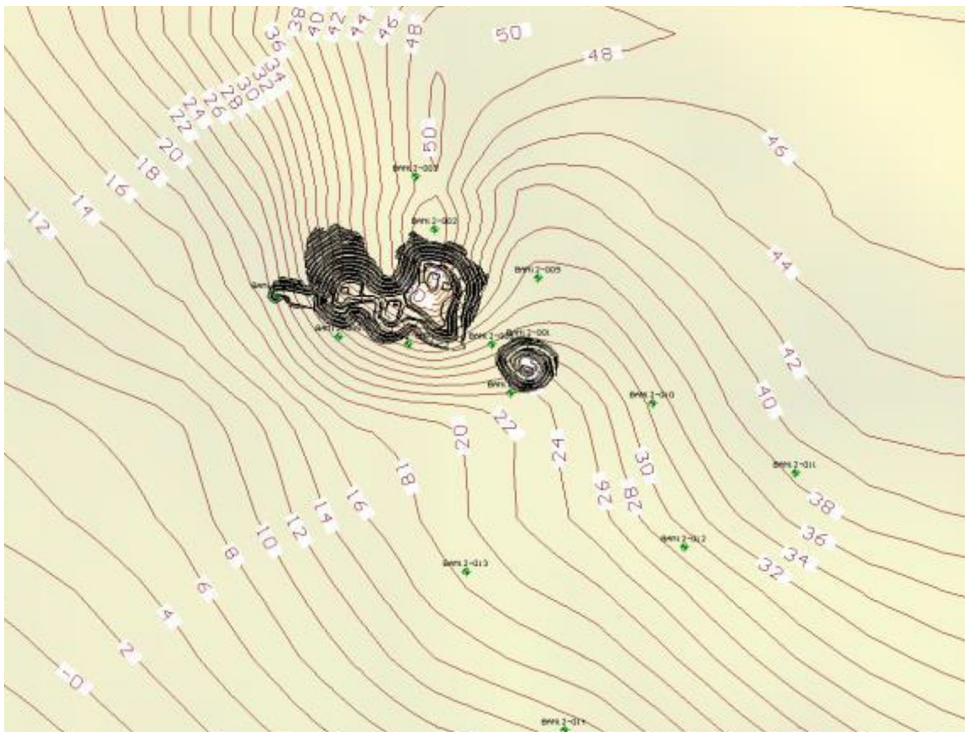

Fig. 6 Contour map of induced post-mining drawdown (m) using AnAqSim modelling

the pit), due to the major fractures acting as a barrier for the regional groundwater flow.

Discussion and Conclusions

A regional water table aquifer exists hosted in secondary permeability strata with a steep gradient of 0.08 to 0.02 to the south. Under steady state conditions, the likely pit inflow is on the order of 0.3 to 10.5 L/s. Based on the assessed small groundwater inflow estimate, it is unlikely that advanced pit dewatering will be required, unless currently unknown major fractures are intersected by the pit. Some short-term groundwater inflow can be expected as the developing pit intersects fractured aquifers in the rock mass, but these inflows should rapidly decrease as the water in aquifer storage is irrevocably depleted.

The strategy for the dewatering of the pit walls would involve horizontal drill holes in the pit wall to dewater isolated pockets of groundwater that could destabilise the batter slope. Pore pressure in the pit walls should be relieved by passive drainage or by the use of horizontal drains. Vertical wells are unlikely to be successful, except in discrete local areas. In-pit basal sumps and pumps

should be sufficient to remove water from the pit floor, especially in the warmer summer months, and these will be useful in case there is severe water quality deterioration. During winter, the in-pit water and groundwater in the fractures directly behind the pit wall may freeze. Horizontal drains in the pit slopes may be required to decrease structural instability.

The change in storage value (Scenario 2: Table 3) showed that there will be minor gain (302, 350 m^3/year), which is about 2 m in pit lake height. Due to evaporation losses, the pit lake will remain shallow. It is likely that the lake will not exceed a depth of 2 m under steady-state conditions; however, stormwater influxes may temporarily increase the pit water depth.

The current study demonstrated that it is possible to use existing analytical models and available aquifer hydraulic information to resolve practical pit water management in a future open cast mining scenario and to provide a snapshot of information to decision makers, provided that the model flaws and limitations are thoroughly understood. These analytical models should not be used in scenarios where the field conditions and the underlying assumptions are not well understood, because the blind use of these equations could lead to inaccurate and potentially misleading results.

Acknowledgments The authors thank Bill Colvin and the staff of Bayan Airag Exploration LLC for providing permission to publish this work and in the undertaking of the fieldwork. The manuscript has benefitted from the reviewers' and editors' comments.

References

Barker JA (1988) A generalized radial flow model for hydraulic tests in fractured rock. Water Resour Res 24(10):1796–1804

Battumur (2009) Assessment of Water Supply Options for Proposed Bayan Airag Gold-Copper Mine. Report: January 2009

Bredehoeft J (2005) The conceptualization model problem-surprise. Hydrogeol J 13:37–46

Dragoni W (1998) Some consideration regarding the radius of influence of a pumping well. Perugia, Italy. http://www.unipq.it/~denz/Dragoni.pdf

Fitts CR (2010) Modeling aquifer systems with analytic elements and subdomains. Water Resour Res 46:W07521. doi:10.1029/2009WR008331

Hasiniaina F, Zhou J, Guoyi L (2010) Regional assessment of groundwater vulnerability in Tamtsag Basin, Mongolia using drastic model. J Am Sci 6(11):65–78

Kazemi GA (2012) Hydrogeology—A Global Perspective. InTech Publ Co, Rijeka, ISBN 978-953-51-0048-5

Li W, Liu Z, Guo H, Li N, Kang W (2011) Simulation of groundwater fall caused by geological discontinuities. Hydrogeol J 19:1121–1133

Marinelli F, Niccoli, WL (2000) Simple analytical equations for estimating ground water inflow to a mine pit. Groundwater 38(2):311–314

Mengistu H, Tessema A, Abiye T, Demlie M, Lin H (2015) Numerical modeling and environmental isotope methods in integrated mine-water management: a case study from the Witwatersrand basin, South Africa. Hydrogeol J 23(3):533–550

Rapanova N, Grmela A, Vojtek D, Halir J, Michalek B (2007) Groundwater flow modelling applications in mining hydrogeology. Mine Water Environ 26:264–270

Rupp DE, Schmidt J, Woods RA, Bidwell VJ (2009) Analytical assessment and parameter estimation of a low-dimensional groundwater model. J Hydrol 377:143–154

Sellers PJ, Meeson BW, Closs J, Collatz J, Corprew F, Hall FG, Kerr Y, Koster R, Kos S, Mitchell K, McManus J, Myers D, Sun KJ, Try P (1995) An overview of the ISLSCP Initiative I global Data Sets, ISLSCP Initiative I Global Data Sets for Land–Atmosphere Models, CD-ROM, Vol 1–5, NASA

Singh VP, Woolhiser DA (2002) Mathematical modelling of watershed hydrology. J Hydrol Eng 7:270–292

Sloan WT (2000) A physics-based function for modelling transient groundwater discharge at the watershed scale. Water Resour Res 36:225–242

SMEC (2011) Bayan Airag Gold Project Pre-Feasibility Level Mine Water Supply Assessment. For: Bayan Airag Exploration LLC

SMEC (2012) Bayan Airag Gold Project Feasibility Level Mine Water Supply Assessment. For: Bayan Airag Exploration LLC

Soni AK, Sahoo LK, Ghosh UK (2015) Importance of radius of influence and its estimation in a limestone quarry. J Inst Eng D 96(1):77–83

Tammetta P (2013) Estimation of the height of complete groundwater drainage above mined longwall panels. Groundwater 51(5):723–734

Toran L, Bradbury KR (1988) Groundwater flow model of drawdown and recovery near an underground mine. Groundwater 26(6):724–733

Vandenbohede A, Hinsby K, Courtens C, Lebbe L (2011) Flow and transport model of a polder area in the Belgian coastal plain: example of data integration. Hydrogeol J 19:1599–1615

Voss CI (2011) Groundwater modelling fantasies-part 1, adrift in the details. Hydrogeol J 19:1281–1284

Wu JC, Zeng XK (2013) Review of the uncertainty analysis of groundwater numerical simulations. Chin Sci Bull 58:3044–3052. doi:10.1007/s11434-013-5950-8

Yihdego Y, Danis C, Paffard A (2015) 3-D numerical groundwater flow simulation for geological discontinuities in the Unkheltseg Basin, Mongolia. Environ Earth Sci J 73(8):4119–4133. doi:10.1007/s12665-014-3697-4